CONF-850175--1

LA-UR-85-942

LA-UR--85-942

DE85 010108

Los Alamos National Laboratory is operated by the University of California for the United States Department of Energy under contract W-7405-ENG-36

TITLE AN ADAPTIVE REZONER IN A TWO-DIMENSIONAL LAGRANGIAN HYDRODYNAMIC CODE

AUTHOR(S) J. J. Pyun, X-7
J. S. Saltzman, X-7
A. J. Scannapieco, X-7
A. Carroll, X-7

SUBMITTED TO 4th In'l Conf. on Numerical Methods in Laminar and Turbulent Flow, Swansea, England, July 8-12, 1985

DISCLAIMER

Los Alamos Los Alamos National Laboratory
Los Alamos, New Mexico 87545

FORM NO 836 R4

AN ADAPTIVE REZONER IN A TWO-DIMENSIONAL LAGRANGIAN HYDRODYNAMIC CODE

J. J. PYUN, J. S. SALTZMAN,
A. J. SCANNAPIECO, D. CARROLL

Theoretical Application Division
Computation Physics Group
Los Alamos National Laboratory
Los Alamos, New Mexico, USA

ABSTRACT

In an effort to increase spatial resolution without adding additional meshes, an adaptive mesh was incorporated into a two-dimensional Lagrangian hydrodynamics code along with two-dimensional flux corrected (FCT) remapper.

The adaptive mesh automatically generates a mesh based on smoothness and orthogonality, and at the same time also tracks physical conditions of interest by focusing mesh points in regions that exhibit those conditions; this is done by defining a weighting function associated with the physical conditions to be tracked.

The FCT remapper calculates the net transportive fluxes based on a weighted average of two fluxes computed by a low-order scheme and a high-order scheme. This averaging procedure produces solutions which are conservative and nondiffusive, nd maintains positivity.

This adaptive rezoner package was modularized such that users can add the adaptive mesh to any logical regions bounded by slip/collapse lines. Extensive

calculations of various test problems were performed, and the results of these calculations will be discussed in detail.

1. INTRODUCTION

The purpose of this paper is to describe an adaptive rezoner incorporated into the two-dimensional (2D) finite difference Lagrangian hydrodynamic (hydro) code with a quadrilateral cell. This 2D hydro code is a FORTRAN program for the Cray-1 Computer designed to calculate the time-dependent solutions of two-dimensional hydrodynamic problems with elastic and plastic flow including phase transition and spall in plane or cylindrical geometry. A quarilateral cell is formed by two adjacent constant I lines and two adjacent constant J lines. An overall code architecture including its finite difference equations, is given in references 1 and 2.

In section 2 of this papers, a variational method for the automatic mesh generation in a two-dimension [3] is developed. First, a formulation of the functional for generating adaptive meshes is described. Then the Euler equations for this fuctional are derived, and the finite difference approximations to the Euler equations are solved by iteration. A two-dimensional (2D) FCT (flux corrected transport) remapper [4] is developed in section 3. First, an algorithm for calculating a low-order flux and high order flux with corner-coupling is given. Then a method for limiting fluxes, and the final antidiffusive transport steps are briefly described. Several test problems including a reactive HE (high explosive) burn were calculated using this code with adaptive meshes. Some results of these calculation are given section 4.

2. VARIATION METHOD FOR MESH GENERATION

It is well known that there are two approaches to increase a spatial resolution of the finite difference approximations to the time-dependent partial differential equations without using finer uniform meshes over the whole mesh system. One is the use of a stationary mesh system with the mesh refinement in space to obtain the desired accuracy at the proper locations. The other is the use of an automatic mesh generation scheme to move the mesh points in such a way that they concentrate at the places where they are needed most for higher resolution. Researchers along the first approach are exemplified by the multigrid methods for Brant et al., [6,7] and the local mesh refinement Method of Berger et al., [8]. The second approach is the variational method for moving mesh points of Brackbill and Saltzman [3], and Ianenko et al., [9]. The variational method of Brackbill and Saltzman was used in this paper.

The methods of multigrid and local mesh refinement can

achieve high local accuracy, but they lose the numerical accuracy and stability at the boundary between fine and coarse mesh regions. Since their mesh systems are not boundary-fitted, complicated interpolations necessary for the problems with shocks and complex geometry. On the other hand, the control mechanism in the variational methods of Yanenko, Brackbill, and Saltzman is more problem-oriented, e.g., the velocities of the moving mesh points, the distortion in the mesh and concentration of the mesh points can be controlled almost independently by varying different control parameters in the functionals to be minimized.

The detailed description of the variational formulation of the mesh generator of Brackbill and Saltzman is elaborated in reference 3. Therefore, only its brief description will be given in this section.

2.1 Variational Formulation of the Mesh Generator

Consider a map from the two-dimensional parameter space $x(\xi,\eta)$ to $x(i,j)$, and we define the following functionals which measure the properties of the map:

$$I_1 = \int_D |(\nabla\xi)^2 + (\nabla\eta)^2| \, dV, \qquad (1)$$

$$I_2 = \int_D (\nabla\xi \cdot \nabla\eta)^2 \, dV, \qquad (2)$$

$$I_3 = \int_D wJ \, dV, \qquad (3)$$

$$J = \frac{\partial x}{\partial \xi}\frac{\partial y}{\partial \eta} - \frac{\partial x}{\partial \eta}\frac{\partial y}{\partial \xi}, \qquad (4)$$

where (ξ,η) are continuous variables which take on integer values, (i,j) are the indices which give the location of mesh vertices $x(i,j)$, $w(x,y)$ is a given function of x and y, J is the Jacobian of the map.

The integral in equation (1) measure the smoothness of the mapping from (ξ,η) to (x,y). In particular, the gradients in the integrand measures the spacing of the constant ξ and η lines. It seems pausible that a mesh that has smooth changes in spacing would have a functional value less than a jaggedly spaced mesh. We will call this integral the smoothness functional. The intergral in equation (2) measures the orthogonality of constant ξ and η lines. If the mesh were perfectly orthogonal then the integral would be zero. We will call this integral the orthogonality functional. The integral in equation (3) measures how well the volume elements are conforming to a given weight function $w(x,y)$. If we were to

minimize this integral, we would predict that where w is large J should be small and conversely where J is large w should be relatively small. Further, if J is small in a neighborhood of some point P then the grid should have many points close together in a neighborhood of the point P. We will call this last integral the volume weighting functional.

Then, we take a linear combination of the integrals as below. The lambdas are all chosen positive and their relative size determines the importance given to each integral.

$$I = I_s + \lambda_v I_v + \lambda_o I_o. \tag{5}$$

2.2 Euler Equations for the Variational Problem

The Euler equations for the smooth functional I_s is are:

$$b_{s1}x_{\xi\xi} + b_{s2}x_{\xi\eta} + b_{s3}x_{\eta\eta} + a_{s1}y_{\xi\xi} + a_{s2}y_{\xi\eta} + a_{s3}y_{\eta\eta} = 0$$

and (6)

$$a_{s1}x_{\xi\xi} + a_{s2}x_{\xi\eta} + a_{s3}x_{\eta\eta} + c_{s1}y_{\xi\xi} + c_{s2}y_{\xi\eta} + c_{s3}y_{\eta\eta} = 0.$$

where

$$\begin{aligned} a_{s1} &= -A\alpha, & b_{s1} &= B\alpha, & c_{s1} &= C\alpha, \\ a_{s2} &= 2A\beta, & b_{s2} &= -2B\beta, & c_{s2} &= -2C\beta, \\ a_{s3} &= -A\gamma, & b_{s3} &= B\gamma, & c_{s3} &= C\gamma. \end{aligned} \tag{7}$$

$$A = x_\xi y_\xi + x_\eta y_\eta, \qquad B = y_\xi^2 + y_\eta^2, \qquad C = x_\xi^2 + x_\eta^2. \tag{8}$$

$$\alpha = (x_\eta^2 + y_\eta^2)/J^2, \qquad \beta = (x_\xi x_\eta + y_\xi y_\eta)/J^2, \qquad \gamma = (x_\xi^2 + y_\xi^2)/J^2. \tag{9}$$

The Euler equations for the orthogonality functional I_o are:

$$b_{o1}x_{\xi\xi} + b_{o2}x_{\xi\eta} + b_{o3}x_{\eta\eta} + a_{o1}y_{\xi\xi} + a_{o2}y_{\xi\eta} + a_{o3}y_{\eta\eta} = 0$$

(10)

$$a_{o1}x_{\xi\xi} + a_{o2}x_{\xi\eta} + a_{o3}x_{\eta\eta} + c_{o1}y_{\xi\xi} + c_{o2}y_{\xi\eta} + c_{o3}y_{\eta\eta} = 0.$$

with coefficients

$$\begin{aligned} a_{o1} &= x_\eta y_\eta, & b_{o1} &= x_\eta^2, & c_{o1} &= y_\eta^2, \\ a_{o2} &= x_\xi y_\eta + x_\eta y_\xi, & b_{o2} &= 2(x_\xi x_\eta + y_\xi y_\eta), & c_{o2} &= 2(x_\xi x_\eta + y_\xi y_\eta), \\ a_{o3} &= x_\xi y_\xi, & b_{o3} &= x_\xi^2, & c_{o3} &= y_\xi^2. \end{aligned} \tag{11}$$

Finally, the Euler equations for the volume weighting functional I_v are

$$2w(b_{i1}x_{\xi\xi} + b_{i2}x_{\xi\eta} + b_{i3}x_{\eta\eta} + a_{i1}y_{\xi\xi} + a_{i2}y_{\xi\eta} + a_{i3}y_{\eta\eta}) = -J^2\frac{\partial w}{\partial x}$$

and (12)

$$2w(a_{i1}x_{\xi\xi} + a_{i2}x_{\xi\eta} + a_{i3}x_{\eta\eta} + c_{i1}y_{\xi\xi} + c_{i2}y_{\xi\eta} + c_{i3}y_{\eta\eta}) = -J^2\frac{\partial w}{\partial y},$$

where the coefficients are given by

$$\begin{aligned} a_{i1} &= -x_\eta y_\eta, & b_{i1} &= y_\eta^2, & c_{i1} &= x_\eta^2, \\ a_{i2} &= x_\xi y_\eta + x_\eta y_\xi, & b_{i2} &= -2y_\xi y_\eta, & c_{i2} &= -2x_\xi x_\eta, \\ a_{i3} &= -x_\xi y_\xi, & b_{i3} &= y_\xi^2, & c_{i3} &= x_\xi^2. \end{aligned} \tag{13}$$

Three sets of Euler equations are to be added together with coefficients given by

$$\begin{aligned} a &= a_3 + \lambda_1 a_1 + \lambda_0 a_0, \\ b &= b_1 + \lambda_1 b_1 + \lambda_0 b_0, \\ c &= c_3 + \lambda_1 c_1 + \lambda_0 c_0. \end{aligned} \tag{14}$$

The resulting system of elliptic equations are numerically solved by the classical Gauss-Jacobi iteration.

3. THE TWO-DIMENSIONAL FCT REMAPPER

Lagrangian hydrodynamics calculations are sometimes terminated prematurely because of severe distortions in the computational cell. Then, there is the need to change the computational cell in order to continue the calculation. Or the computational mesh has to be changed to satisfy various criteria if an adaptive mesh algorithm is used with the Lagrangian hydrodynamics calculations. It is then necessary to transfer the conserved quantities (such as mass, momentum, and energy) from the old mesh to the new mesh. This process is called remapping or rezoning. In essence, it is an interpolation procedure from one mesh to another. However, we would like to impose three important restrictions on this process; namely we want it to be conservative, nondiffusive and positive.

The FCT remapper used in this paper was developed by Scannapieco [4] and Zalesak [10]. The detailed description of FCT remapper is elaborated in references 4 and 10. Therefore, only its brief description will be given here.

The basis for the new remapper is a flux corrected transport technique developed by Zalesak for fixed Eulerian meshes. Zalesak's technique had to be modified to run on an arbitrary quadrilateral mesh. This meant that the high and

low order fluxes used in the technique had to be defined on an arbitrary quadrilateral mesh.

The basic philosophy of the FCT technique is that two algorithms are used to carry out the transport of the fluid quantities: An algorithm low-order, in space, that is highly diffusive but gives smooth results, is combined through the medium of a flux-limiter with a high-order algorithm that is very nondiffusive but causes ripples in the solution. The combination produces an algorithm that is accurate to any desired to order in space, is nondiffusive, and does not cause numerical ripples. Since the FCT remapper is written flux conservative form, it conserves all transported quantities to machine roundoff, and maintains positivity.

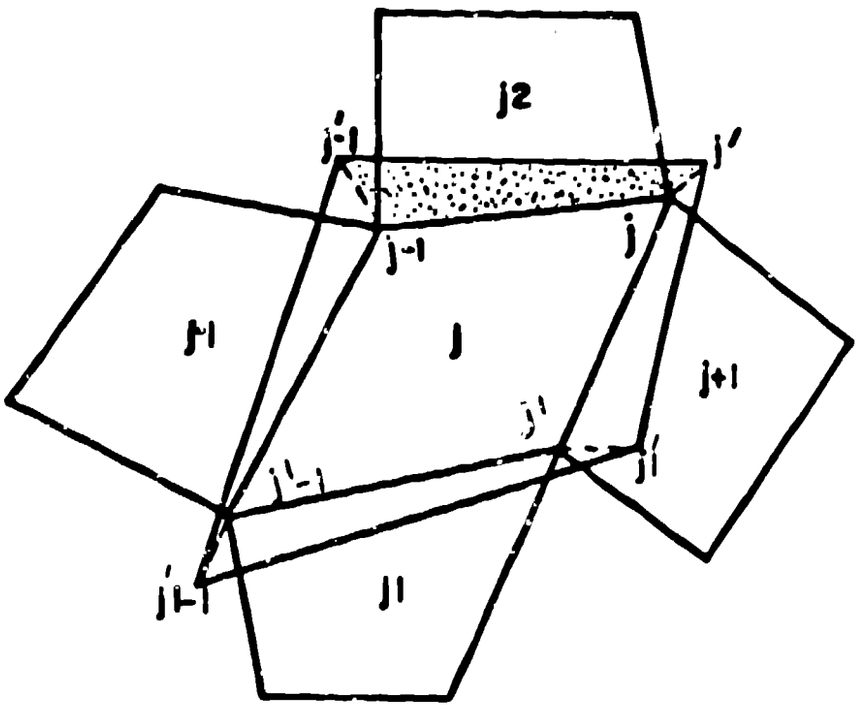

Fig. 1 Calculation of Noncorner-Coupled Low-Order Fluxes

Now we will describe how to calculate the lower-order fluxes. Fig. 1 shows two overlapping quadrilateral Lagrangian meshes and their vertices j, $j-1$, $j'-1$, j', j', $j'-1$, $j''-1$, and j''. The unprimed quantities refer to the old mesh and the primed quantities refer to the new mesh. The lower-order fluxes are calculated by donor cell (or upwind) difference scheme assuming the conserved quantities are piecewise constant over the old and new cells. For

example, the low-order flux between the meshes j and j^2 is calculated by multiplying a displaced cell volume associated with a dotted area in Fig. 1 and a conserved quantity from a donor-cell.

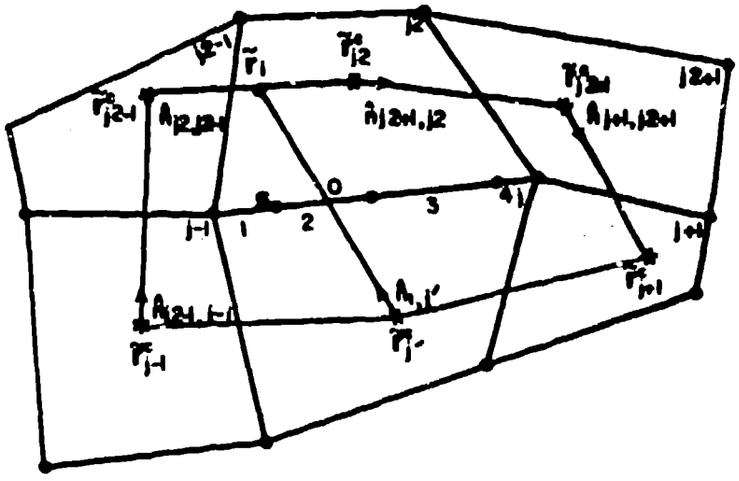

Fig. 2 Calculations of Corner-Coupled High-Order Fluxes.

To calculate the corner-coupled high-order fluxes, we construct a hypothetical cell j and its five neighbor cells j-1, j^2- 1, j^2, J^2 + 1 and j +1 as shown in Fig. 2. The vertex of this hypothetical cell is located at the average position between the old and new cell vertices. Then, the conserved quantities are linearly interpolated along the top side panel between the hypothetical cell j and its five neighbor cells. Finally, the corner-coupled high-order fluxes along the topside panel are calculated by taking the line integration of the advective terms. The corner-coupled higher-order fluxes along the rightside panel are calculated in a similiar way.

Since we calculated the low-order and high-order fluxes, we are ready to calculated the conserved quantities in the new mesh as below:

1. Define the antidiffusive flux,

$$A_j = F_{HJ} - F_{LJ} \tag{15}$$

where F_{Hj} is a net high-order flux away from a new cell j

F_{Lj} is a net low-order flux away from a new cell j.

2. Compute the conserved quantities in the new cell using the low-order fluxes,

$$Q^{L}_{Nj} = Q_{oj} - F_{Lj}/V_{oj} \tag{16}$$

where Q^{L}_{Nj} is the conserved quantities in the new cell j using the low-order fluxes,

Q_{oj} is the conserved quantities in old cell j.

V_{oj} is the volume of the old cell j.

3. Limited the A_j in a manner such the Q^{L}_{Nj} as computed in step 4 below is free of extrema found in Q^{L}_{Nj} or Q_{oj},

$$A^{c}_{j} = c_j A_j, \quad 0 \leq c_j \leq 1 \tag{17}$$

4. Apply the limited antidiffusive fluxes,

$$Q_{Nj} = Q^{L}_{Nj} - A^{c}_{j}/V_{oj} \tag{18}$$

where Q_{Nj} is final conserved quantities in the new cell j.

Zalesak's flux limiter [10] was used in this paper.

4. Results, Discussions, and Conclusion

Figs 3 and 4 show comparisons of 2D Hydro Code calculations for the shock test problem at the same time, with or without the adaptive mesh update.

The test problem has two layers of hollow metal balls which are made of a high density material. An ideal gas with gamma of 5/3 was sandwiched between two hollow balls. Two strong shocks whose strengths are approximately 1 Megabar, are generated along two forty-five degree lines from the North and South poles, and these two shocks move azimuthally toward the equator.

The adaptive mesh was only added on the ideal gas region,

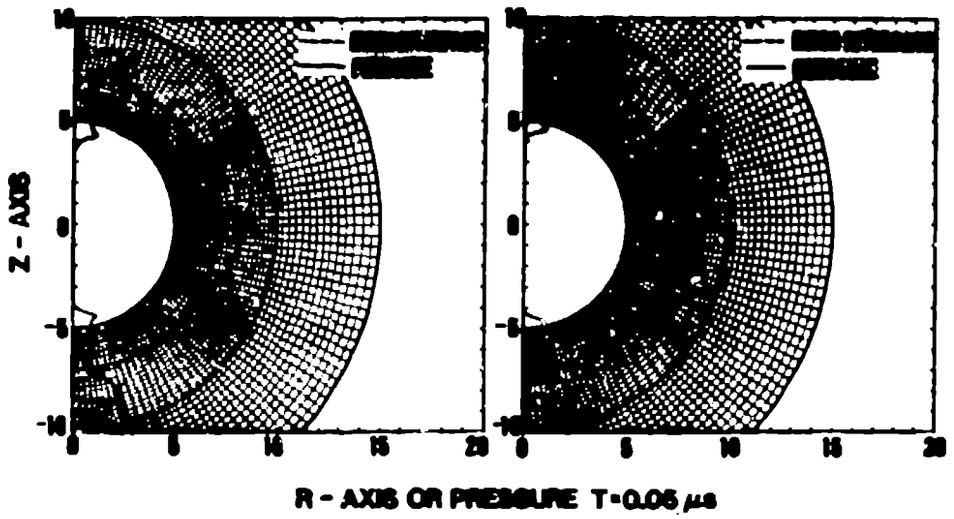

Fig. 3-a

Fig. 4-a

Comparisons of Two Azimuthally-Moving Shocks Calculations Using 2D Hydro Code with (Fig. 3) or without (Fig. 4) Adaptive Mesh.

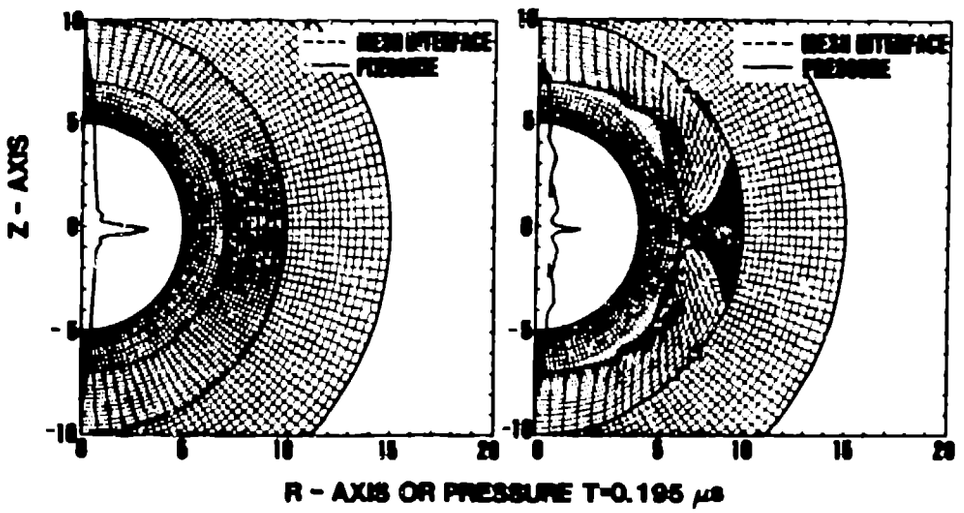

Fig. 3-b

Fig 4-b

Comparisons of Two Azimuthally-Moving Shocks Calculations Using 2D Hydro Code with (Fig.3) or without (Fig. 4) Adaptive Mesh.

and both the smooth functional as well as the volume weignting functional was turned on. The purpose of the smooth functional is to connect fine and coarse mesh regions with smoothly increasing or decreasing meshes. On the other hand,

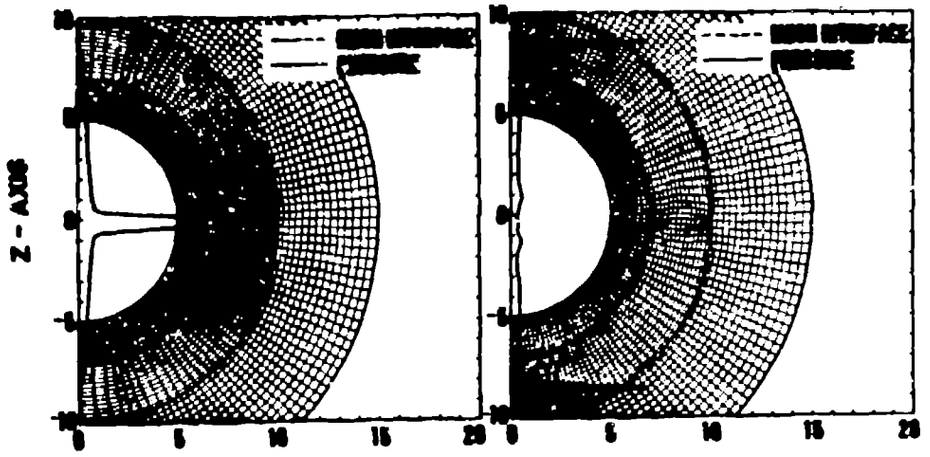

Fig. 3-c Fig. 3-d

Calculations of Two Azimuthally-Moving Shocks ofter their Collisions at the Equator Region using 2D Hydro Code with Adaptive Mesh.

the purpose of the volume functional is to resolve a certain physical variable associated with a function (e.g., a shock) by adding fine meshes, and to follow this physical variable. The physical variable to be followed in our test problem is a pressure gradient.

The mesh interface and the shock pressure vs. the Z-directional distance are plotted together with the same scale. Figs. 3-a and 4-a show that two shock fronts move azimuthally toward the equator. Please, note how closely the adaptive mesh follows the shock front. In addition, the fine and coarse mesh regions are connected smoothly by increasing or decreasing meshes. Figs 3-b and 4-b show the results of mesh interfaces and shock pressure profiles at approximately 0.195 microseconds when two shocks collide with each other, forming a Mach stem. Two-dimensional Hydro Code without the adaptive mesh update, died at this time because of mesh tanglings. However, 2D Hydro Code with the adaptive mesh kept calculating the transient behaviors of two shocks as shown in Figs. 3-c and 3-d. The maximum shock strength attained approximately 6.5 Megabars at about 0.21 microseconds at the equator.

Then, two shocks moved back to the polar axis and were reflected at about 0.382 microseconds.

Now we will use the adaptive mesh for calculations of reactive HE burns. The test problem has a cylindrical geometry, and has one detonation point surrounded by a

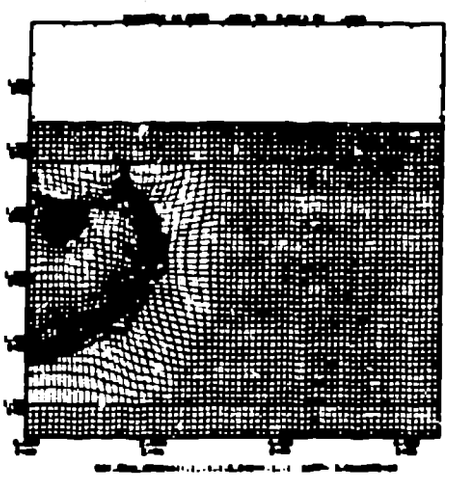

Fig. 5-a

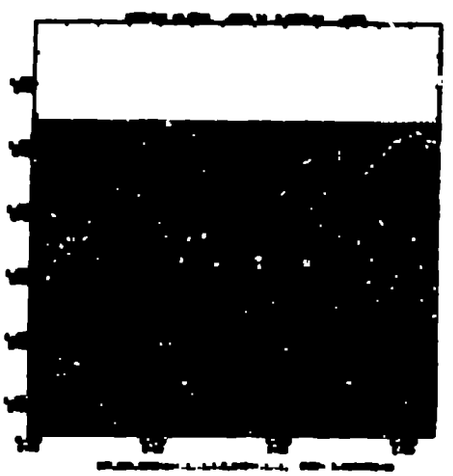

Fig. 6-a

Comparisons of Forest Fire Reactive HE Burn Calculations Using 2D Hydro Code with (Fig. 5) or without (Fig. 6) Adaptive Mesh.

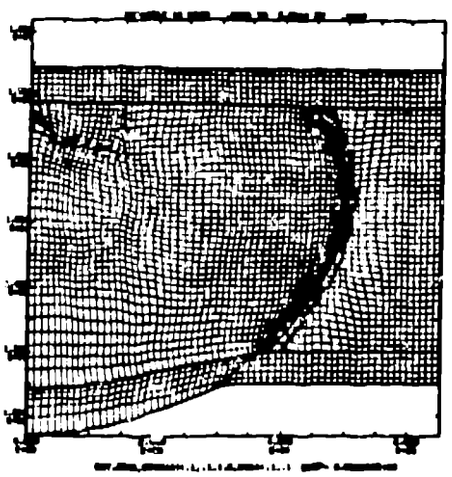

Fig. 5-b

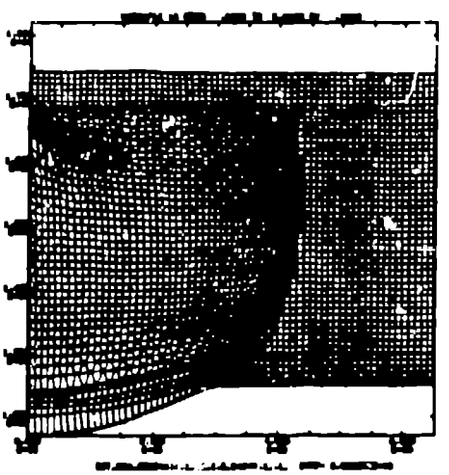

Fig. 6-b

Comparisons of Forest Fire Reactive HE Burn Calculations Using 2D Hydro Code with (Fig. 5) or without (Fig. 6) Adaptive Mesh.

sensitive HE and a rectangular inert foam material at the top-left side. An entire HE device was enclosed by two aluminum

plates at the top and bottom sides.

Figs. 5, and 6 show comparison of 2D Hydro Code calculations for the reactive HE test problem at the same time, with and without adpative mesh update.

The mesh interface and unburned HE mass fraction contour were plotted together with the same scale in Figs. 5 and 6. The heavy solid lines in Figs. 5 through 6 indicate the boundary line between the burned and unburned HE. The adaptive mesh was only added on the HE and inert foam material regions. The smooth functional, the volume functional, and the orthogonal functional were turned on. The physical variable to be followed in our test problem in a pressure gradient.

Figures 5 and 6 show how the detonation front moves with time. Please, note how closely the adaptive meshes follow the detonation front in Fig. 5. In addition, the fine and coarse mesh regions are connected by smoothly increasing or decreasing meshes as shown in Fig. 5. Therefore, Fig. 5 shows a relatively narrow detonation front without any hourglass and finger-like instabilites behind. However, Fig. 6 shows both hourglass and finger-like instabilities behind and at detonation front. Two-dimensional Hydro Code without the adpative mesh died at about 6.05 microseconds because of hourglass instabilities. 2D Hydro Code with and without the adaptive mesh calculated the detonation velocity is 0.89 and 0.78 cm/microseconds, respectively. The theoretical detonation velocity is 0.89 cm/microseconds.

Two major obstacles preventing a successful calculation of reactive HE burns using the adaptive mesh have been tendency of a mesh adjuster to pull most of meshes from a region ahead of a detonation front to a detonation front region and a mix of a partially-burned HE cell with an unburned HE cell by a remapper The former makes the mesh adjuster run out of meshes at the region ahead of the detonation front, and the latters results in artificial burning of the HEs, making the detonation front move faster than its theoretical velocity. To cure these problems, the displacements of mesh points which pack the meshes close to the detonation front, are calculated by a linear weighting of two displacements, that is, one by calculated by the mesh adjuster, and the other by multiplying a local fluid velocity and a timestep. Since the local fluid velocity is zero at the region ahead of the detonation front, this linear weighting of two displacement tends to make the mesh adjuster pull more meshes from the region behind the detonation front rather than ahead of the detonation front which, in turn, makes the remapper less likely mix the partially-burned HE cell with the unburned HE cell.

The main thrust of this work has been to implement the adaptive rezoning capability into the code, and we are now beginning to use it, in particular, for calculations for reactive HE burns. These are preliminary results and do not represent the word.

We plan to incorporate the more advanced rezoner [5] into 2D Hydro Code as part of an effort to cure the artificial burning of the HEs. This rezoner was developed by John Dukowicz and maintains the second-order accuracy in space.

In conclusion, the adaptive mesh can handle intractable problems, and increases the spatial resolution of the physical variables without adding additional mesh.

5. REFERENCES

1. Blewett, P.J. "Stress Calculations in MAGEE Difference Form," LA-4601-MS, 1971.

2. Orr, S.R., Elliott, R.L., and Pequette, E.C., "MAGEE Code," Los Alamos National Laboratory internal report, 1971.

3. Brackbill, J.U., and Saltzman, J.S., "Adaptive zoning for Singular Problems in Two Dimensions," J. Comput., Phys. vol. 46, p.342, 1982.

4. Scannapieco, A.J., "An Automatic Rezoner for Lagrangian Quadrilateral Hydrocodes," LA-UR-82-2897, 1982.

5. Dukowicz, J.K., Conservative Rezoning (Remapping) for General Quadrilateral Meshes," J. Comput. Phys., vol.54, p.411, 1984.

6. Brant, A. "Multi-Level Adaptiave Solution to Boundary-Value Problems," Math. Comput., Vol. 33, SP.333, 1977.

7. Alcouffe, R. G., et al., "The Multi-Grid Method for the Diffusion Equation with Strongly Discontinuous Coefficients," LA-UR-80-1463, 1980.

8. Berger, M., et al., "Grid Generation for Time-Dependent Problems: Criteria and Methods," Numerical Grid Generation Tech., NASA Conf. Pub. #2166, p.181, 1981.

9. Yanenko, N.N., et al., "A Moving-Grids Difference Scheme for Solving the Equations for a Viscous Gas," U.S.S.R Comput. Maths. Math. Phys., vol, 19, p.178, 1979.

10. Zalesak, S.T., "Fully Multidimensional Flux-Corrected Transport Algorithms for Fluids," J. Comput, Phys., vol. 31, p.335, 1979.